Optical Response of Sr_2RuO_4 Reveals Universal Fermi-Liquid Scaling and Quasiparticles Beyond Landau Theory

D. Stricker,[1] J. Mravlje,[2] C. Berthod,[1] R. Fittipaldi,[3] A. Vecchione,[3] A. Georges,[4,5,1] and D. van der Marel[1]

[1]*Département de Physique de la Matière Condensée, Université de Genève,*
24 quai Ernest-Ansermet, 1211 Genève 4, Switzerland
[2]*Jožef Stefan Institute, Jamova 39, Ljubljana 1000, Slovenia*
[3]*CNR-SPIN, and Dipartimento di Fisica "E. R. Caianiello", Universita di Salerno,*
I-84084 Fisciano (Salerno) Italy
[4]*Collège de France, 11 place Marcelin Berthelot, 75005 Paris, France*
[5]*Centre de Physique Théorique, École Polytechnique, CNRS, 91128 Palaiseau, France*

We report optical measurements demonstrating that the low-energy relaxation rate $(1/\tau)$ of the conduction electrons in Sr_2RuO_4 obeys scaling relations for its frequency (ω) and temperature (T) dependence in accordance with Fermi-liquid theory. In the thermal relaxation regime, $1/\tau \propto (\hbar\omega)^2 + (p\pi k_B T)^2$ with $p = 2$, and ω/T scaling applies. Many-body electronic structure calculations using dynamical mean-field theory confirm the low-energy Fermi-liquid scaling and provide quantitative understanding of the deviations from Fermi-liquid behavior at higher energy and temperature. The excess optical spectral weight in this regime provides evidence for strongly dispersing "resilient" quasiparticle excitations above the Fermi energy.

Liquids of interacting fermions yield a number of different emergent states of quantum matter. The strong correlations between their constituent particles pose a formidable theoretical challenge. It is therefore remarkable that a simple description of low-energy excitations of fermionic quantum liquids could be established early on by Landau [1], in terms of a dilute gas of "quasiparticles" with a renormalized effective mass, of which ^{3}He is the best documented case [2,3].

Breakdown of the quasiparticle concept can be observed in the transport of metals tuned onto a quantum phase transition, but Fermi-liquid (FL) behavior is retrieved away from the quantum-critical region [4,5]. The relevance of FL theory to electrons in solids is documented by a number of materials, such as transition metals [6], heavy-fermion compounds [7], and doped semiconductors [8]. Among transition-metal oxides, Sr_2RuO_4 is a remarkable example which has been heralded as the solid-state analogue of ^{3}He [9] for at least three reasons: remarkably large and clean monocrystalline samples can be prepared, transport properties display low-temperature FL characteristics [10], and there is evidence for p-wave symmetry of its superconducting phase [11], as in superfluid ^{3}He.

FL theory makes a specific prediction for the universal energy and temperature dependence of the inelastic lifetime of quasiparticles: Because of phase-space constraints imposed by the Pauli principle as well as momentum and energy conservation, it diverges as $1/\omega^2$ or $1/T^2$ [1,5]. More precisely, the inelastic optical relaxation rate is predicted to vanish according to the scaling law

$1/\tau \propto (\hbar\omega)^2 + (p\pi k_B T)^2$, with $p = 2$ [12–14]. This leads to universal ω/T scaling of the optical conductivity $\sigma(\omega)$ in the thermal regime $\hbar\omega \sim k_B T$ [14]. Surprisingly, however, despite almost 60 years of research on Fermi liquids, this universal behavior of the optical response and especially the specific statistical factor $p = 2$ relating the energy and temperature dependence have not yet been established experimentally [13–17].

Here, we report optical measurements of Sr_2RuO_4 with 0.1 meV resolution [18,19] which reveal this universal FL scaling law [20]. We establish experimentally the universal value $p = 2$ and demonstrate remarkable agreement between the experimental data and the theoretically derived scaling functions in the FL regime. Importantly, the identification of the precise FL response also enables us to characterize the deviations from FL theory. The manifestation of these deviations in our data is an excess spectral weight above 0.1 eV. We show that this is an optical fingerprint of the abrupt increase in dispersion of "resilient" quasiparticle excitations. This confirms the recent prediction [21] on the basis of dynamical mean-field theory (DMFT) that well-identified peaks in the spectral function persist far above the asymptotic low-energy and low-temperature Landau FL regime where the relaxation rate has a strict ω^2 dependence. In this Letter, we perform realistic DMFT calculations for Sr_2RuO_4 which yield excellent agreement with the measured optical spectra. There are three bands at E_F: a two-dimensional one (γ) of d_{xy} character and two quasi-1D bands (α and β), respectively [9]. We show that the deviations from FL behavior in

the optical spectra are caused by resilient quasiparticle (QP) excitations associated with unoccupied states, which are inaccessible in usual photoemission experiments.

Optical spectroscopy is a powerful probe of—among other things—the subtle low-energy behavior of electron liquids. Earlier optical studies of Sr_2RuO_4 have reported that the in-plane low-energy spectral weight is about 100 times larger than the one along the c axis, with an onset below 25 K of a T^2 relaxation rate [22–24]. The lowest-lying interband transitions, located above 1 eV, have been previously identified as d-d transitions [25]. In the optical conductivity of Sr_2RuO_4 this is revealed as a peak at 1.7 eV ([26], Table I). In the range displayed in Fig. 1, $\sigma(\omega)$ is entirely due to the free carrier response. The dynamical character of the inelastic scattering can be captured by a frequency-dependent memory function $M(\omega)$ as described in Ref. [27] so that

$$\sigma(\omega) = \frac{i\epsilon_0\omega_p^2}{\omega + M(\omega)}. \qquad (1)$$

On the other hand, an intraband optical absorption process excites electron-hole *pairs*, with the consequence that the optical relaxation rate $M_2(\omega)$ is proportional to $(\hbar\omega)^2 + (p\pi k_B T)^2$ with the value $p = 2$ [12–14]. The optical conductivity is then characterized by a narrow Lorentzian-like zero-frequency mode (Drude peak), followed by a (non-Drude) "foot" at $\hbar\omega \approx 2\pi k_B T$ [14]. Hence, the signature of FL theory and of the frequency dependence of $1/\tau$ is actually a *deviation from Drude's form* (corresponding to a constant τ).
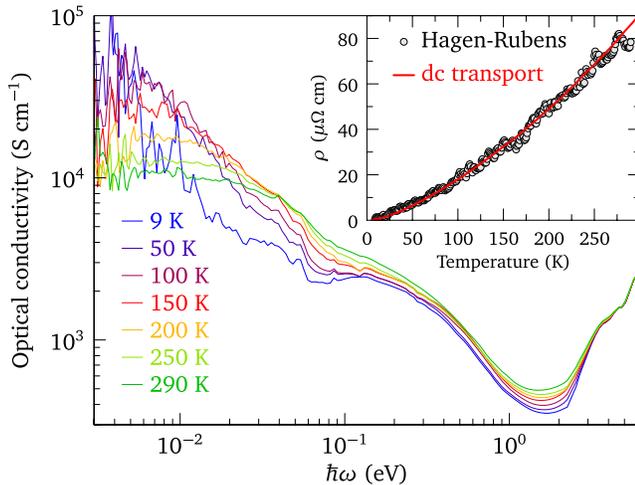

FIG. 1 (color online). Real part of the optical conductivity of Sr_2RuO_4 for selected temperatures between 9 and 290 K. Inset: Zero-frequency resistivity determined by the Hagen-Rubens fit of the reflectivity (open circles) and four-terminal dc resistivity of the same crystal (solid red curve) multiplied with a factor 0.84, which is within the range of geometrical factors due to sample shape and contact layout.

Several recent optical studies have reported ω^2 and T^2 for $M_2(\omega)$ in a number of different materials. However, in neither of these cases does the coefficient p match the prediction $p = 2$: $p \sim 1$ in URu_2Si_2 [16], $p \sim 2.4$ in the organic material BEDT-TTF [28], and $p \sim 1.5$ in underdoped $HgBa_2CuO_{4+\delta}$ [17]. One possible scenario that has been proposed to explain this discrepancy is the presence of magnetic impurities [13]. We decided instead to look at the $4d$ correlated material Sr_2RuO_4 which can be synthesized in very pure form, with well-established T^2 resistivity below 25 K [9].

The Sr_2RuO_4 crystal employed for this work was grown by using the traveling floating zone technique [29]. The quality of the crystal was confirmed by different techniques [30] with a superconducting transition at 1.4 K. The ab-plane crystal surface of 5.1×3.6 mm^2 was micropolished and cleaned prior to transferring the sample to the UHV cryostats for optical spectroscopy. Near-normal reflection reflectivity spectra in the range from 2 meV to 3 eV were collected between 290 and 9 K at a cooling rate of 1 K per minute. The optical conductivity obtained by Kramers-Kronig analysis is shown in Fig. 1 for a few selected temperatures. The close match of the dc resistivity and $\rho(T) = \lim_{\omega\to 0} 1/\sigma_1(\omega, T)$ (inset in Fig. 1) provides evidence that the low-frequency optical data are accurate at all temperatures.

The optical conductivity displayed in Fig. 1 is dominated by the peak centered at zero frequency, corresponding to the optical response of the free charge carriers. Upon lowering the temperature from 290 to 9 K, this peak becomes extremely narrow, and its maximum at $\omega = 0$ increases by 2 orders of magnitude. The weak features at 40, 57, and 85 meV correspond to optical phonons. The standard Drude model assumes a frequency-independent relaxation rate. The frequency dependence of $M_2(\omega)$ shown in Fig. 2(b) is therefore manifestly non-Drude-like and signals the presence of a dynamical component in the quasiparticle self-energy. Moreover, below 0.1 eV, $M_2(\omega)$ has a positive curvature for all temperatures corresponding to ω^η with $\eta \approx 2$ ([26], Sec. III), and $M_1(\omega)$ has a linear frequency dependence that is only weakly changing with temperature. This is the expected behavior in a Fermi liquid. The low-frequency mass enhancement factor $m^*(\omega)/m = 1 + M_1(\omega)/\omega$ varies from 3.3 at 9 K to 2.3 at 290 K. The $m^*(\omega)/m$ curves ([26], Sec. II) fall slightly below the one of a previous room temperature study [31].

In order to reveal the signature of Fermi-liquid behavior, we searched for the presence of a universal scaling of the form $M_2(\omega, T) \propto \xi_p^2 \equiv (\hbar\omega)^2 + (p\pi k_B T)^2$ in the data, by plotting $M_2(\omega, T)$ parametrically as a function of ξ_p^2 for different choices of p and calculating the root-mean square (rms) deviation of this plot from a straight line. The frequency range used in this analysis was limited to $\hbar\omega \leq 36$ meV, and the largest temperature considered, T_{max}, was allowed to vary down to $T_{max} = 35$ K, below
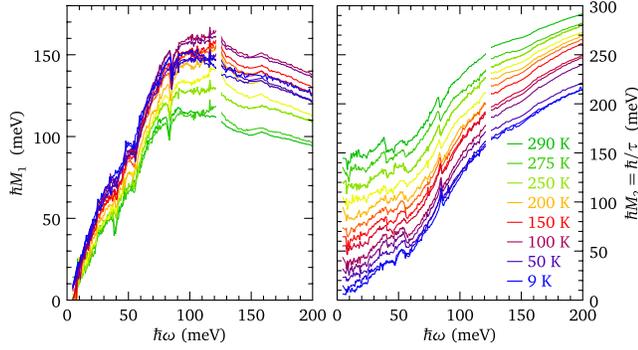
FIG. 2 (color online). Real part (left) and imaginary part (right) of the Sr_2RuO_4 memory function for selected temperatures between 9 and 290 K. A white space is introduced near 130 meV where data sets from different detectors were linked.

which the fitted temperature range becomes too small to produce reliable output. The result of the scaling collapse for $p = 2$ and $T \leq T_{max} = 40$ K is displayed in Fig. 3. The rms minimum for each T_{max} defines p^*, shown as a
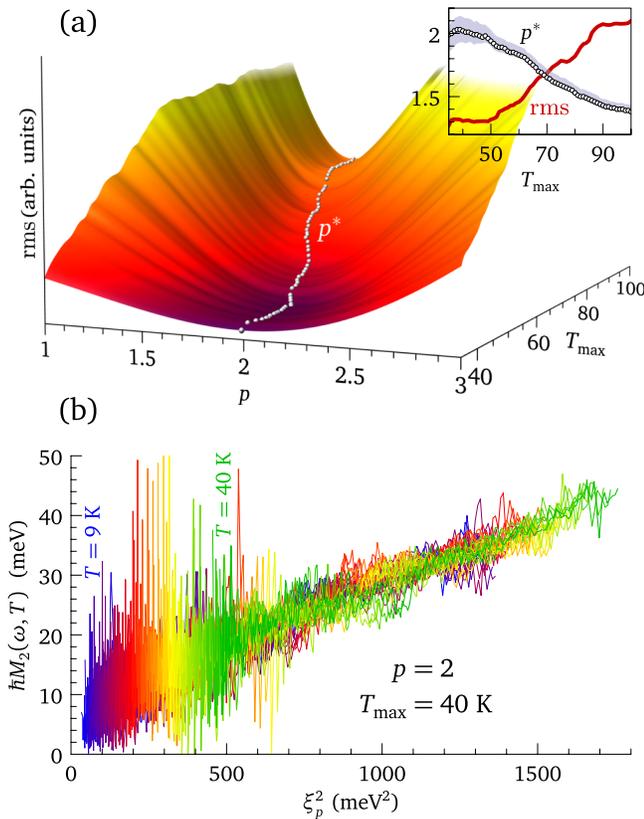

FIG. 3 (color online). (a) Root-mean square deviation of the relaxation rate $M_2(\omega, T)$ from a linear dependence in ξ_p^2, for $\hbar\omega \leq 36$ meV and $T \leq T_{max}$, as a function of p and T_{max}. The inset shows the value p^* and the rms at the minimum versus T_{max}. A value $p^* = 2$ is found below $T_{max} \sim 40$ K. The shaded region shows how p^* changes if the frequency range is varied by ± 5 meV. (b) Collapse of the relaxation rate data for $T \leq 40$ K.

function of T_{max} in the inset. When the range T_{max} is varied from 100 to 35 K, we observe a flow from $p = 1.5$ towards the plateau value $p = 2$, which is approached for $T_{max} \leq 50$. This confirms the expectation of a flow towards universal Fermi-liquid behavior for $T \to 0$, for which we expect a collapse of all data on a universal function of ξ_p with $p = 2$. A similar analysis conducted on the raw reflectivity data leads to the same conclusion that $p = 2$ ([26], Sec. III).

A direct confirmation of FL behavior is found in the optical conductivity curves (Fig. 4). They exhibit a characteristic non-Drude feature in perfect agreement with the universal FL response. This feature is an increase of conductivity with respect to the low-frequency Drude response around the thermal frequency $\hbar\omega = 2\pi k_B T$, appearing most clearly as a shoulder in a log-log plot. The universal FL response, including impurity scattering, has been parametrized by only three temperature-independent parameters [14]. This three-parameter model can reproduce the low-frequency optical conductivity data of Sr_2RuO_4 in the whole temperature range below 40 K, where $p = 2$, as illustrated in Fig. 4.

For energies above 0.1 eV and/or temperatures above 40 K, the measured conductivities clearly depart from the reference FL (Fig. 4). All deviations go in the direction of a larger conductivity (both real and imaginary parts), in particular, in the 0.1–0.5 eV energy range. In order to understand the origin of this increased conductivity, we have calculated the optical spectra within an *ab initio* framework that combines density-functional theory (DFT) with the many-body DMFT [32], as described in [33,34] and applied to Sr_2RuO_4 in [35]. The bare dispersions and velocities are obtained from DFT for the three t_{2g} bands, and the local (momentum-independent) DMFT self-energies for each orbital are calculated by using the same interaction parameters as in previous works ([26], Sec. IV). The theoretical results are presented in Fig. 4 as circles. The overall shapes of experimental data and theoretical DMFT results match closely, and satisfactory agreement is also found for absolute values (note that the comparison in Fig 4 involves no scale adjustment). At low frequency and temperature, the *ab initio* calculations show a Drude peak and a thermal shoulder, in excellent agreement with the experimental data and with the FL model. The differences at the lowest frequencies can be attributed to impurity scattering, included in the FL model but not in the DMFT calculation, in order to keep the latter parameter-free. More interestingly, above 0.1 eV the theory deviates from the FL model in precisely the same manner as the experiment does. At higher temperatures, while the predictions extrapolated from the low-temperature FL severely underestimate the conductivity, the agreement between DFT + DMFT and experiments remains excellent in the 0.1–0.5 eV range. The calculated imaginary part of the optical conductivity is systematically somewhat lower than the experimental data.
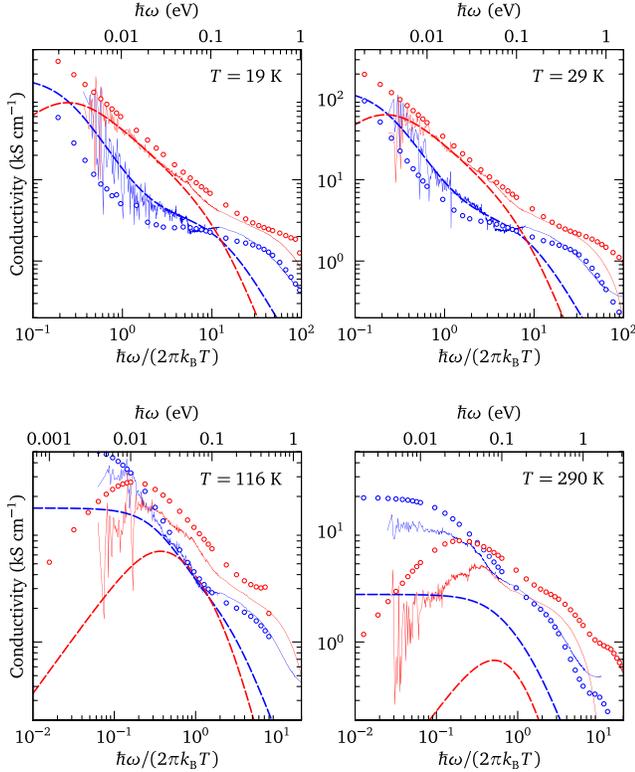
FIG. 4 (color online). Comparison of the experimental optical conductivity (solid lines), Fermi-liquid model (dashed lines), and DFT+DMFT calculation (circles) at selected temperatures. The real and imaginary parts of the conductivity are shown in blue and red, respectively. The three parameters of the Fermi-liquid model, including impurity scattering, are fit to the experimental data in the range $\hbar\omega \leq 36$ meV and $T \leq 40$ K. The DFT+DMFT calculation ignores impurity scattering.

The difference increases with temperature and is most clear for 290 K. Electron-phonon interactions in fact cause additional mass enhancement, which leads to a suppression of both σ_1 and σ_2 for $\omega \to 0$ and an increase of optical conductivity in the phonon energy range. This effect is not included in the DMFT calculations and may explain the remaining differences with experimental data.

We have carried out a series of numerical experiments in order to elucidate the origin of the non-FL excess of optical spectral weight in the 0.1–0.5 eV frequency range ([26], Sec. IV). First, we eliminated band-structure effects as a possible cause. The band structure enters the optical conductivity via a transport function $\Phi(\varepsilon)$, proportional to the average of the squared velocities at a given energy. This function is smooth, unlike the density of states which diverges at the van Hove singularity of the xy band. Indeed, we have verified that the replacement of $\Phi(\varepsilon)$ by its Fermi-surface value $\Phi(0)$ causes no significant change in the theoretical curves of Fig. 4. The excess spectral weight is therefore due to electronic correlations and must be linked to a structure in the single-particle self-energies.

The imaginary part of the self-energies follows the FL parabolic dependence at low energy but starts to deviate already well below 0.1 eV in the direction of a weaker scattering. In particular, between +0.2 and +0.4 eV, still in the domain of intraband transitions, the scattering rate goes through a maximum and decreases slightly at higher energy. A similar phenomenon with a saturation of the scattering rate was observed in the single-band Hubbard model and was shown to give rise to resilient QPs [21]. In Sr_2RuO_4, the signature of resilient QPs is even more striking: It is signaled by a *drop* of the scattering rate for empty states above $\sim$0.35 eV. Consistent with Kramers-Kronig relations, this drop implies a sharp minimum in the real part of the self-energy which is found in the energy range 0.1–0.15 eV. As a consequence, QPs above this energy scale have velocities *larger* than the bare velocities. In the theoretical spectral function, these appear as peaks which are broader than the low-energy Landau QP peaks and have a very steep dispersion in the range 0.2–0.4 eV, leading to an inverted waterfall-like structure.

These resilient QPs with large velocities are the source of excess spectral weight and deviation from FL behavior above 0.1 eV. Indeed, optical spectroscopy is sensitive to these excitations above the Fermi level, since it probes transitions between occupied and unoccupied states. The abrupt increase of QP velocities predicted by DFT+DMFT results in a maximum in the real part of the calculated memory function $M_1(\omega)$ in the range 0.1–0.2 eV, hence providing an explanation for the corresponding feature found experimentally (Fig. 2). We also note that more subtle changes in QP dispersions (kinks) at $\sim$30 meV, previously found in both angle-resolved photoemission spectroscopy (ARPES) [19,36] and DMFT [35], are also visible in M_1 and M_2 at lower energy but do not change the frequency dependence of the optical conductivity so strikingly.

The resilient QP excitations above the Fermi level predicted by our calculations and leading to the sharp feature in M_1 are not directly accessible to conventional ARPES, which probes only occupied states. Recently, two-photon ARPES has been shown to provide energy and momentum-resolved information on unoccupied states [37], and we propose that our theoretical results ([26], Fig. SM14) could be put to the test in the future by using this technique for Sr_2RuO_4.

In summary, we have performed reflectance and ellipsometry measurements for a Sr_2RuO_4 single crystal in a wide range of frequencies and temperatures and observed for the first time the universal optical signatures of the Landau quasiparticles in a FL. The low-energy optical relaxation rate obeys $(\hbar\omega)^2 + (p\pi k_B T)^2$ scaling with $p = 2$, and the optical conductivity exhibits a pronounced non-Drude foot at the thermal frequency $\hbar\omega = 2\pi k_B T$. The identification of a low-energy FL regime provides a reference to characterize without ambiguity the deviations from FL theory. In

Sr_2RuO_4, the most significant deviation at low temperature is an increase of conductivity developing above 0.1 eV. With the help of DFT + DMFT calculations, we ascribed the extra spectral weight to resilient quasiparticle excitations above the Fermi level, i.e., relatively broad but still strongly dispersing particlelike excitations with a lifetime differing from the Landau low-energy form. This work demonstrates that optical spectroscopy is a powerful tool to diagnose non-FL behavior, with the provision that the proper FL behavior is taken as the "placebo" reference, instead of the Drude law that is often used for that purpose.

[1] L. Landau, Zh. Eksp. Teor. Fiz. **30**, 1058 (1956).
[2] G. Baym and C. Pethick, *Landau Fermi-Liquid Theory—Concepts and Applications* (Wiley-VCH, New York, 2004).
[3] A. J. Leggett, Rev. Mod. Phys. **76**, 999 (2004).
[4] S. Sachdev, *Quantum Phase Transitions* (Cambridge University Press, Cambridge, England, 1998).
[5] M. Čubrović, J. Zaanen, and K. Schalm, Science **325**, 439 (2009).
[6] M. J. Rice, Phys. Rev. Lett. **20**, 1439 (1968).
[7] K. Kadowaki and S. B. Woods, Solid State Commun. **58**, 507 (1986).
[8] D. van der Marel, J. L. M. van Mechelen, and I. I. Mazin, Phys. Rev. B **84**, 205111 (2011).
[9] A. P. Mackenzie and Y. Maeno, Rev. Mod. Phys. **75**, 657 (2003).
[10] N. E. Hussey, A. P. Mackenzie, J. R. Cooper, Y. Maeno, S. Nishizaki, and T. Fujita, Phys. Rev. B **57**, 5505 (1998).
[11] C. Kallin, Rep. Prog. Phys. **75**, 042501 (2012).
[12] R. N. Gurzhi, Sov. Phys. JETP **35**, 673 (1959).
[13] D. L. Maslov and A. V. Chubukov, Phys. Rev. B **86**, 155137 (2012).
[14] C. Berthod, J. Mravlje, X. Deng, R. Žitko, D. van der Marel, and A. Georges, Phys. Rev. B **87**, 115109 (2013).
[15] D. N. Basov, R. D. Averitt, D. van der Marel, M. Dressel, and K. Haule, Rev. Mod. Phys. **83**, 471 (2011).
[16] U. Nagel, T. Uleksin, T. Rõõm, R. P. S. M. Lobo, P. Lejay, C. C. Homes, J. S. Hall, A. W. Kinross, S. K. Purdy,

[17] S. I. Mirzaei, D. Stricker, J. N. Hancock, C. Berthod, A. Georges, E. van Heumen, M. K. Chan, X. Zhao, Y. Li, M. Greven, N. Barišić, and D. van der Marel, Proc. Natl. Acad. Sci. U.S.A. **110**, 5774 (2013).
[18] T. E. Kidd, T. Valla, A. V. Fedorov, P. D. Johnson, R. J. Cava, and M. K. Haas, Phys. Rev. Lett. **94**, 107003 (2005).
[19] N. J. C. Ingle, K. M. Shen, F. Baumberger, W. Meevasana, D. H. Lu, Z.-X. Shen, A. Damascelli, S. Nakatsuji, Z. Q. Mao, Y. Maeno, T. Kimura, and Y. Tokura, Phys. Rev. B **72**, 205114 (2005).
[20] Note that the resolution in the ARPES studies of Refs. [18,19] was 25 and 14 meV, respectively.
[21] X. Deng, J. Mravlje, R. Žitko, M. Ferrero, G. Kotliar, and A. Georges, Phys. Rev. Lett. **110**, 086401 (2013).
[22] T. Katsufuji, M. Kasai, and Y. Tokura, Phys. Rev. Lett. **76**, 126 (1996).
[23] M. G. Hildebrand, M. Reedyk, T. Katsufuji, and Y. Tokura, Phys. Rev. Lett. **87**, 227002 (2001).
[24] K. Pucher, A. Loidl, N. Kikugawa, and Y. Maeno, Phys. Rev. B **68**, 214502 (2003).
[25] J. S. Lee, Y. S. Lee, T. W. Noh, S.-J. Oh, J. Yu, S. Nakatsuji, H. Fukazawa, and Y. Maeno, Phys. Rev. Lett. **89**, 257402 (2002).
[26] See Supplemental Material at http://link.aps.org/supplemental/10.1103/PhysRevLett.113.087404 for details on the optical spectroscopy, the Drude-Lorentz and Fermi-liquid analyses, and the DFT+DMFT calculations.
[27] W. Götze and P. Wölfle, Phys. Rev. B **6**, 1226 (1972).
[28] M. Dressel, J. Phys. Condens. Matter **23**, 293201 (2011).
[29] M. Udagawa, Y. Yanase, and M. Ogata, J. Phys. Soc. Jpn. **74**, 2905 (2005).
[30] R. Fittipaldi, A. Vecchione, S. Fusanobori, K. Takizawa, H. Yaguchi, J. Hooper, R. Perry, and Y. Maeno, J. Cryst. Growth **282**, 152 (2005).
[31] J. S. Lee, S. J. Moon, T. W. Noh, S. Nakatsuji, and Y. Maeno, Phys. Rev. Lett. **96**, 057401 (2006).
[32] A. Georges, G. Kotliar, W. Krauth, and M. J. Rozenberg, Rev. Mod. Phys. **68**, 13 (1996).
[33] M. Aichhorn, L. Pourovskii, V. Vildosola, M. Ferrero, O. Parcollet, T. Miyake, A. Georges, and S. Biermann, Phys. Rev. B **80**, 085101 (2009).
[34] M. Ferrero, O. Parcollet, and L. Pourovskii, a Toolbox for Research on Interacting Quantum Systems, http://ipht.cea.fr/triqs.
[35] J. Mravlje, M. Aichhorn, T. Miyake, K. Haule, G. Kotliar, and A. Georges, Phys. Rev. Lett. **106**, 096401 (2011).
[36] H. Iwasawa, Y. Yoshida, I. Hase, K. Shimada, H. Namatame, M. Taniguchi, and Y. Aiura, Sci. Rep. **3**, 1930 (2013).
[37] J. A. Sobota, S.-L. Yang, A. F. Kemper, J. J. Lee, F. T. Schmitt, W. Li, R. G. Moore, J. G. Analytis, I. R. Fisher, P. S. Kirchmann, T. P. Devereaux, and Z.-X. Shen, Phys. Rev. Lett. **111**, 136802 (2013).